Pure Appl. Chem., Vol. 71, No. 7, pp. 1215–1226, 1999. Paper 282
Printed in Great Britain.

Thermophysics of advanced engineering materials*

Ron D. Weir

Department of Chemistry & Chemical Engineering, Royal Military College of Canada, PO Box 17000, Stn Forces, Kingston, Ontario K7K 7B4, Canada

Abstract: The requirement for novel materials to perform in hostile environments to include high pressure and temperature is the driving force behind the push in research into advanced materials for engineering applications. To assess their usefulness, it is essential to know the thermodynamic properties of any new material. A complete thermodynamic characterisation must incorporate a determination of the thermophysical properties such as the heat capacity from which the enthalpy, entropy, free energy and structural information can be derived, the thermochemical properties such as enthalpies and free energies of formation, and the thermodynamic stability of the material. The thermodynamic properties of two main groups of materials will be reviewed in this plenary lecture, namely the solid transition metal silicides and the solid transition metal chalcogenides. The transition metal silicides are a well-defined family of compounds M_aSi_b with the metal element M within groups 3 to 11 of the periodic table. Their high degree of stability, resistance to oxidation and great tensile strength, all properties at elevated temperatures, account for their desirability as engineering materials. The transition metal chalcogenides have a general formulation MX_2, where M is a transition metal element and X is a chalcogenide specifically sulfur, selenium or tellurium. Virtually all members of this family of layered compounds are composed of a sheet of metal atoms sandwiched between two sheets of chalcogens. Their stability at high temperatures, ease of one layer sliding over adjacent layers, and their ability to allow intercalation by foreign atoms contribute to the demand for their use. It is not surprising that only limited thermodynamic information is available for these two families as the rapid pace in development of new materials is occurring at a rate faster than the experimentalists can determine their thermodynamic properties.

INTRODUCTION

The progress of mankind during time on earth has been directly of indirectly dependent on materials. Periods of development have been labelled in the archeological record to reflect this as the Stone Age, Iron Age, Bronze Age, etc. During the past 30 years of this century, there has been an unprecedented expansion in the number of new materials and these have entered every aspect of our lives. As the millennium approaches, the '*Revolution in Materials*' shows every sign of a continuation, probably with an increase in the pace of development.

The driving force in this push into advanced engineering materials, perhaps better described as advanced materials for engineering applications, is the requirement for their satisfactory performance: (i) in hostile environments to include high pressure and temperature so as not to be adversely affected by the surroundings, and (ii) in sensitive environments where the material does not adversely affect the surroundings as in living systems. Testament to the voracious appetite for new materials are the

* Lecture presented at the 15th International Conference on Chemical Thermodynamics, Porto, Portugal, 26 July–1 August 1998, pp. 1167–1306.
Correspondence: E-mail: weir-r@rmc.ca

expanding fields of electronics, computers, operations in outer space, energy production and medical science to name a few.

The science of materials aids in the fundamental understanding of the chemistry and physics involved. The engineering builds on this knowledge to design materials to meet specifications, parameters within which the materials must perform. A knowledge of the thermodynamic properties is an essential element in the characterisation of any new material. The significance of the thermodynamics is manifested in several aspects: thermodynamic stability that defines resistance to oxidation and decomposition, the sequence of reaction formation to include the rate determining step and resulting phases, the heats of formation and reaction, the free energies that equal the work the material can produce or the work needed to produce the material, information on molecular motion, disorder and transitions in solids.

The questions that naturally follow include 'which thermodynamic properties are needed?, how accurate must the results be?, what secondary properties can be derived?, what role do modelling and simulation play?'

A complete thermodynamic characterisation must incorporate a determination of the thermophysical properties such as the heat capacity from which can be derived the enthalpy, entropy, free energies and structural information, the thermochemical properties such as the enthalpies and free energies of formation, and the thermodynamic stability of the material. The advantage of measuring the heat capacity as the primary determination is that the heat capacity sees all the sources of the energy that contribute to the total. Appropriate integrations of the heat capacity results in the enthalpies, entropies and free energies from which a host of subsequent information can be derived. In addition, the heat capacity against temperature plot may reveal structural or more subtle transitions in the solid; it will also allow information to be deduced about the vibrational frequency distribution, as well as magnetic and electronic phenomena.

It has been necessary to narrow the enormously wide field of materials for this invited lecture and to that end, two groups of important engineering materials have been selected, namely the solid transition metal silicides and the solid transition metal chalcogenides.

THE TRANSITION METAL SILICIDES (CERAMICS)

The transition metal silicides are a well-defined family of compounds M_aSi_b with the metal M from within groups 3 to 11 of the periodic table to include Ti, V, Cu, Y, Mo, W, Pt. At least 39 pairs of elements are possible and our limited knowledge suggests at least 69 stable compounds at $T = 300\,K$. Accounting for their desirability as engineering materials is their resistance to oxidation and great tensile strength elevated temperatures, and their high degree of stability. Their fusion temperatures span a wide range from 1073 K for Cu_3Si to 2773 K for Ta_3Si. Applications in engineering are in refractory materials specifically furnace windings, heating elements and coatings, in interconnect technology, in semiconductors and in the aerospace industry.

The dearth of information is first noted from the phase diagrams for the family which are incomplete for at least 24 elemental pairs and unknown for all the other pairs. One of the most complete is that of Mn_aSi_b shown in Fig. 1 where at least six forms are defined. While some values of temperature have been estimated and extrapolated, the amount of uncertain information is minimum.

The available thermodynamic information for this family is substantially less than is known about the phase diagrams. The heat capacity is known for only a few alloys above $T = 300\,K$ that allow a calculation of the enthalpy, entropy and free energy but in some cases, the associated experimental errors in technique are higher than is desirable. Below $T = 300\,K$, the heat capacity is virtually unknown and therefore so are the enthalpy, entropy and free energies.

The urgency to obtain thermodynamic properties of W Si_2 and Mo Si_2 led us to undertake a study of their thermodynamic properties to include the determination of the heat capacity. The phase diagram for the W_aSi_b is provided in Fig. 2 in which two stable compounds are shown to exist, viz. W Si_2 and W_5Si_3. The equivalent diagram for Mo_aSi_b is shown in Fig. 3 where three compounds are defined as Mo_3Si, Mo_5Si_3 and Mo Si_2.

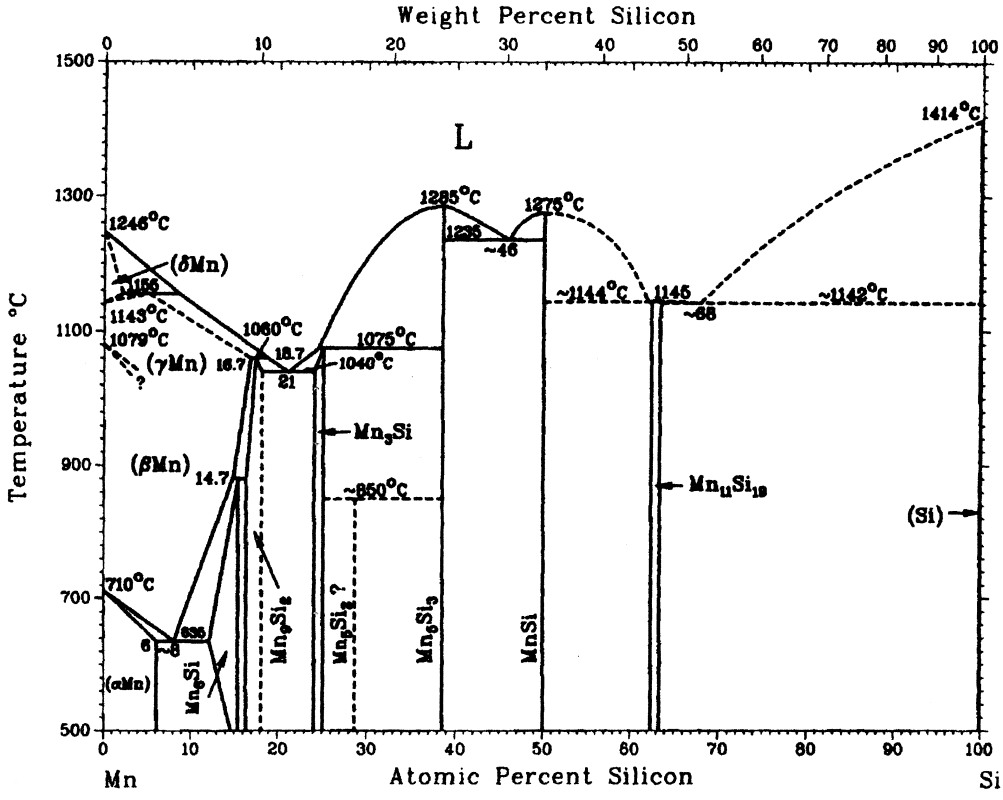

Fig. 1 Phase diagram for Mn-Si with temperature *T* plotted against atomic per cent silicon and weight per cent silicon. The broken lines represent estimated values. Reprinted from [1] with permission. © 1986 ASM International.

THE TRANSITION METAL CHALCOGENIDES

The transition metal chalcogenides have a general formulation M X_2, where M is a transition metal and X is a chalcogenide specifically sulfur, selenium or tellurium. The transition metal lies in groups 4 to 6 of the periodic table to include Ti, Zr, Mo, Ta, W. The 21 pairs of elements in this family are known to produce at least 26 stable compounds at $T = 300$ K. Virtually all members of this family of layered compounds are composed of a sheet of metal atoms sandwiched between two sheets of chalcogens and are often referred to as 2-dimensional materials. Their stability at high temperatures, ease of one layer sliding easily over adjacent layers, and their ability to allow intercalation by foreign atoms contribute to their demand as engineering materials. Even less thermodynamic information is known for this family than is the case for the transition metal silicides.

The phase diagrams are partially known for 11 elemental pairs in this family and unknown for all others. The first member of the chalcogenides studied in our laboratory is W Te_2 with the demand for its use in semiconductors, batteries and as catalysts and solid lubricants at high temperatures. The incomplete phase diagram for the W_aTe_b is shown in Fig. 4 where the fusion temperature is given as $T = (1293 \pm 15)$ K.

RESULTS AND DISCUSSION

The synthesis of W Si_2, Mo Si_2, W Te_2 described in this lecture was a difficult process insofar as pure stoichiometric compounds are concerned. Great care was exercised since small deviations from the expected stoichiometry give rise to significant differences in properties., which in turn makes meaningless any comparison with published results. The materials on which our thermodynamic measurements were carried out are tungsten disilicide W $Si_{2.06}$, molybdenum disilicide Mo $Si_{2.067}$, and tungsten ditelluride W Te_2.

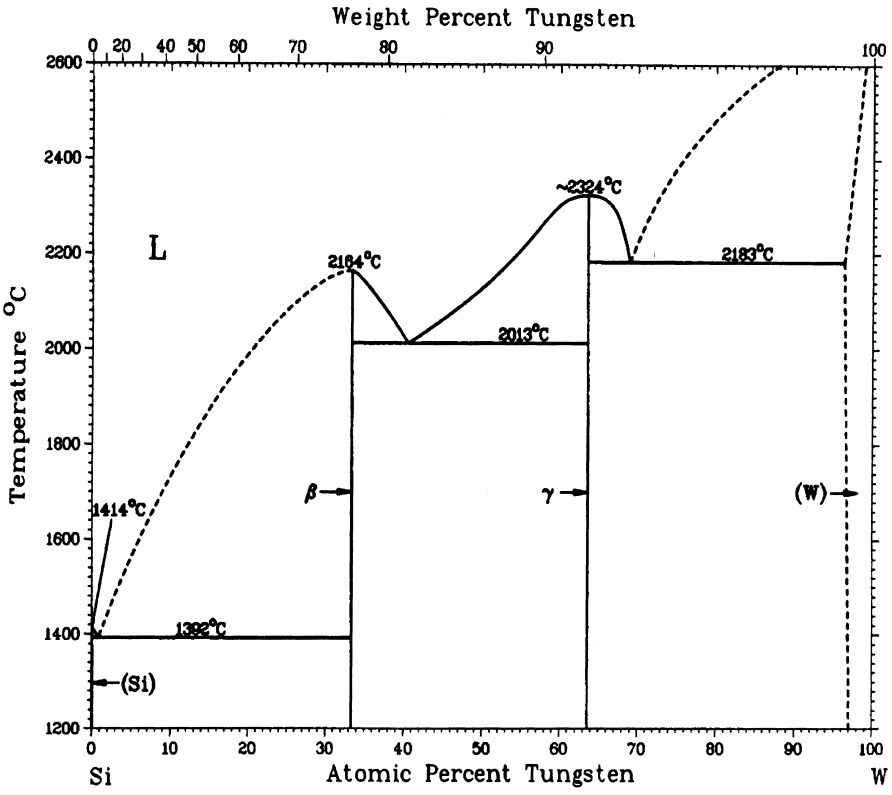

Fig. 2 Phase diagram for Si-W with temperature T plotted against atomic per cent silicon and weight per cent silicon. The broken lines represent estimated values. Reprinted from [1] with permission. © 1986 ASM International

Both tungsten disilicide W $Si_{2.06}$ and molybdenum disilicide Mo $Si_{2.067}$ have a tetragonal structure at $T = 300$ K with space group D^{17}_{4h} [2,3], The molar heat capacity of $WSi_{2.06}$ by adiabatic calorimetry was determined over the interval $5.9 \leq (T/K) \leq 341$ [2]. The heat capacity against temperature curve as the dimensionless $C_{p,m}/R$, where R is the universal gas constant, in Fig. 5, is continuous and without anomalies. The integrations yield S^0_m (cr, 298.15 K) = (68.43 ± 0.17) J/K/mol and ΔG^0_f (cr, 298.15 K) = (79.5 ± 5.5) kJ/mol.

Heat capacities of tungsten disilicide at higher temperatures from drop calorimetry studies have been reported from $461 \leq (T/K) \leq 1068$ [4], and from $1173 \leq (T/K) \leq 2113$ [5]. These are plotted in Fig. 6 together with those for W $Si_{2.06}$ from $5.9 \leq (T/K) \leq 341$ described above. While the characterisation and purity of the samples used in the studies are not described in [4] and [5], it is not unreasonable in view of the phase diagram in Fig. 2 to consider the heat capacity curve continuous to $T = 1200$ K. Therefore the thermodynamic quantities have been evaluated up to $T = 1200$ K [2]. However as a result of the unexpected and unacceptable slope of the heat capacity curve of Bondarenko *et al*. [5] and the fact that the heat capacities at lower temperatures could not be extended smoothly to join the results above $T = 1200$ K, no attempt was made to determine the properties above $T = 1200$ K.

The heat capacities from $7 \leq (T/K) \leq 329$ were measured by adiabatic calorimetry [3] using the identical sample of Mo $Si_{2.067}$ employed for the thermochemical measurements [7]. The heat capacity against temperature plot is shown in Fig. 7 as a smooth curve but with a slight dip or irregularity in the vicinity of $T = 200$ K. This irregularity is thought to be a consequence of the known isotropy in thermal expansion, resistivity and magnetoresistivity in the molybdenum disilicide [8]. The S^0_m (cr, 298.15 K) = (61.48 ± 0.15) J/K/mol.

Other investigators had studied the heat capacity of molybdenum disilicide at temperatures above $T = 350$ K to extend to $T = 2200$ K. These are plotted in Fig. 8, where the heat capacity of the series at low temperatures [3] are contiguous with those of Douglas & Logan [9] and of Walker *et al*. [10]. The lower

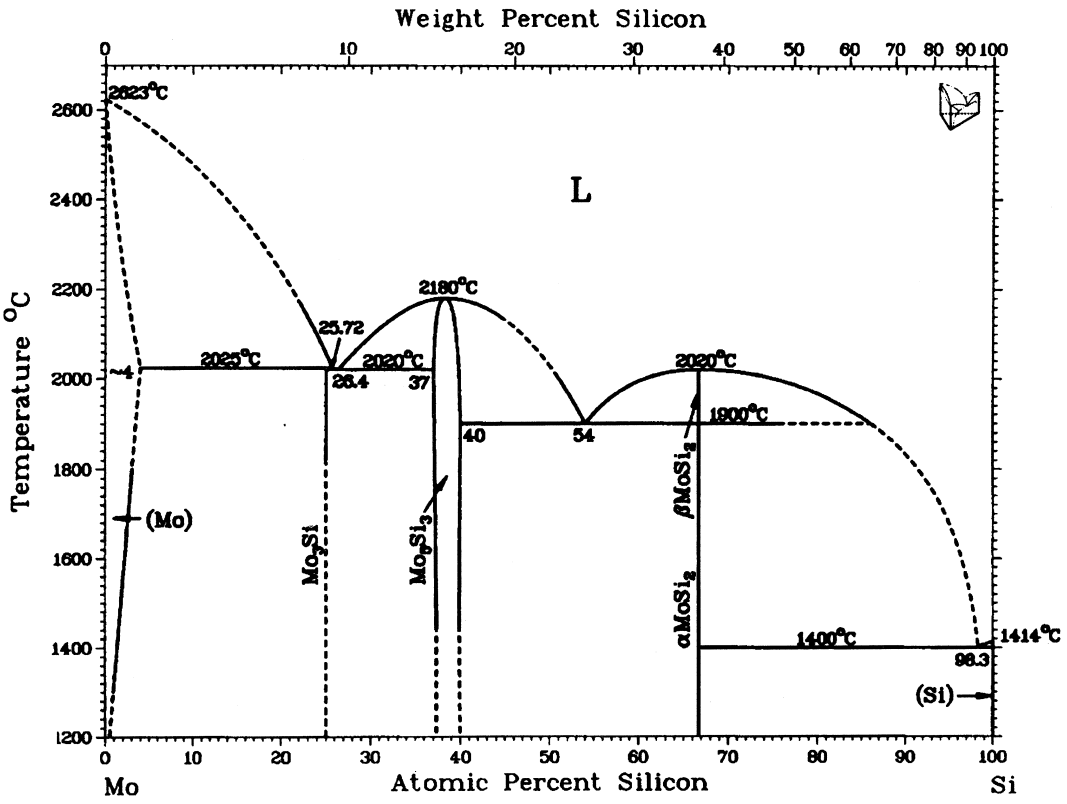

Fig. 3 Phase diagram for Mo-Si with temperature T plotted against atomic per cent silicon and weight per cent silicon. The broken lines represent estimated values. Reprinted from [1] with permission. © 1986 ASM International.

temperature results of Bondarenko *et al*. [11] were made by adiabatic calorimetry and agree with the others up to about $T = 800$ K. However the measurements by Mezaki *et al*. [4] in this region are excluded from Fig. 8 because the slope was unreasonable for a material for which all degrees of freedom are believed to be already activated. The higher temperature results of Bondarenko *et al*. were determined by drop calorimetry using enthalpy increments over the range $1200 \leq (T/\mathrm{K}) \leq 2200$. As evident in Fig. 8, these show an unreasonable slope and the heat capacity at $T = 1200$ K determined by Bondarenko *et al*. [11] via adiabatic calorimetry is 14% higher than that obtained at the same temperature from their work via enthalpy increments.

By means of the functional relationship related to the expected course of the high temperature heat capacities and estimated probabilities, the curve has been extended to about $T = 2200$ K [3] as depicted in Fig. 9. This temperature represents the upper limit for the existence of the tetragonal structure (α-Mo Si_2) of Fig. 3. The experimental molar heat capacities are compared for W Si_2 and Mo Si_2 up to $T = 1200$ K in Fig. 10.

The carefully prepared and analysed sample of tungsten ditelluride, W Te_2 [6] was part of the same sample used for the thermochemical studies by O'Hare [7]. X-ray investigations at room temperature showed the structure to be orthorhombic with space group D^{16}_{2h}, a structure stable to $T = 1493$ K based on the phase diagram in Fig. 4. The molar heat capacity of the W Te_2 was measured by adiabatic calorimetry from $5.5 \leq (T/\mathrm{K}) \leq 329$ and the $C_{p,m}/R$ against temperature curve is shown in Fig. 11.

A broad anomaly is observed between $92 \leq (T/\mathrm{K}) \leq 175$ with the resulting S^0_m (cr, 298.15 K) = (132.70 ± 0.25) J/K/mol, which is about double those for W $Si_{2.06}$ and Mo $Si_{2.067}$. A similar but less prominent anomaly is evident in the heat capacity over the same temperature range for the tungsten diselenide W Se_2 [12], which is shown in Fig. 12.

These effects are reminiscent of even more striking anomalies noted in previous studies of the tetragonal Scheelites viz. NH_4ReO_4, ND_4ReO_4, NH_4IO_4, ND_4IO_4, and the orthorhombic NH_4ClO_4,

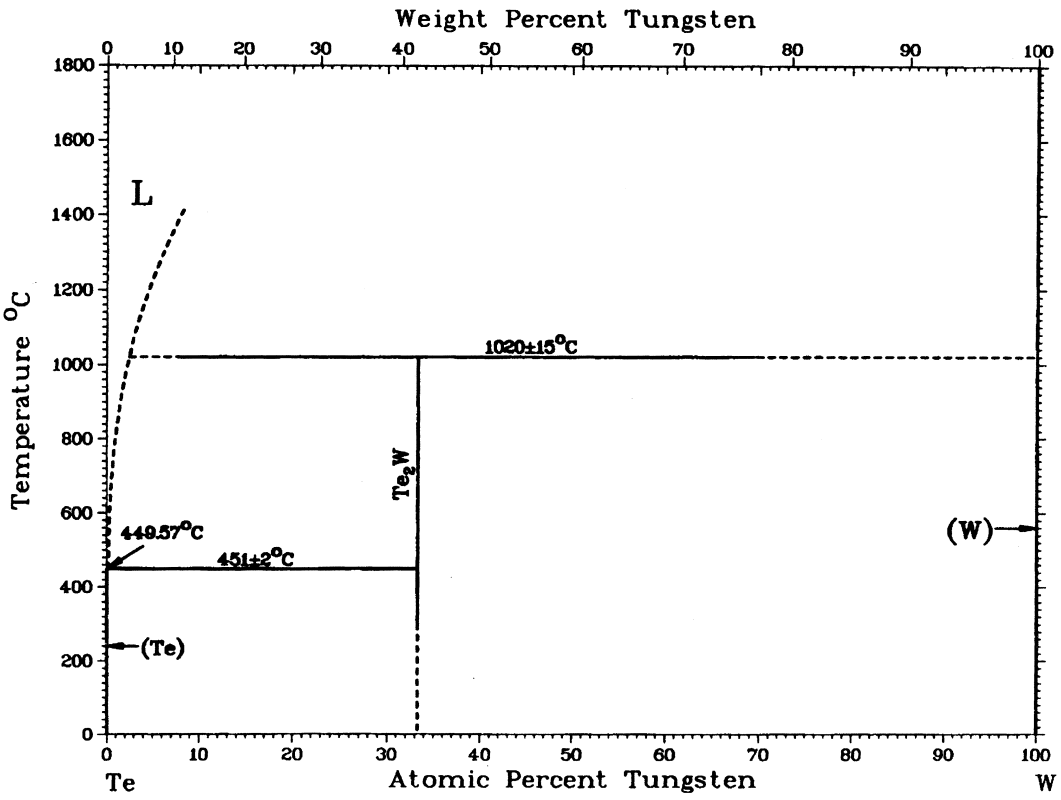

Fig. 4 Phase diagram for Te-Wi with temperature T plotted against atomic per cent silicon and weight per cent silicon. The broken lines represent estimated values. Reprinted from [1] with permission. © 1986 ASM International.

ND_4ClO_4 [13–19], anomalies that appear related to the anisotropic thermal expansion in these compounds.

For the W Si_2, Mo Si_2, and W Te_2, analysis of the heat capacity results reveals an electronic contribution γT that augments the lattice component of the total heat capacity. The lattice contribution

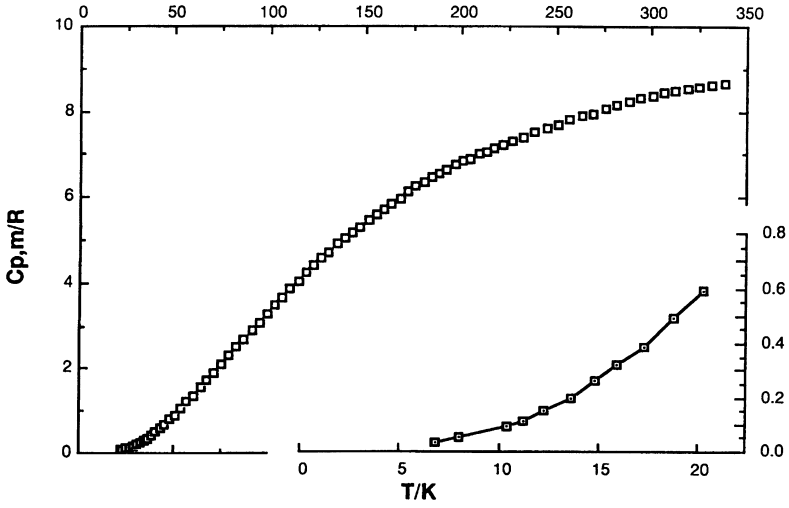

Fig. 5 Experimental molar heat capacities, $C_{p,m}/R$, at constant pressure plotted against temperature T for $WSi_{2.06}$. The region below $T = 22$ K is enlarged in the lower right-hand corner.

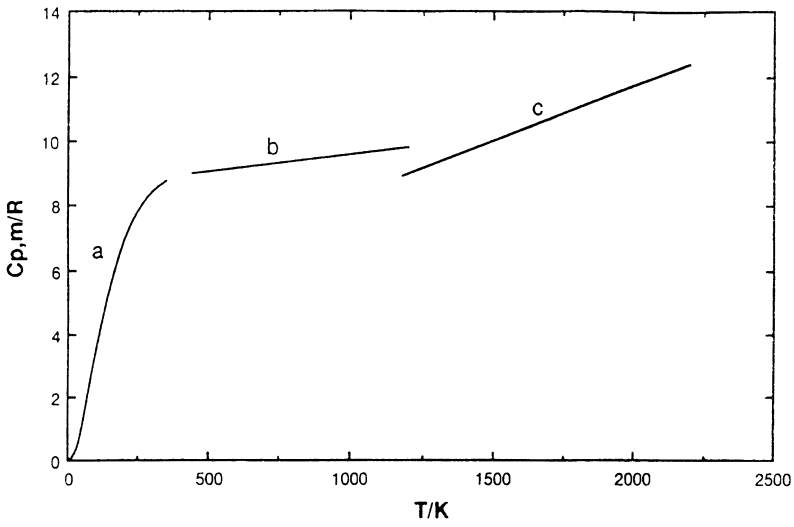

Fig. 6 Experimental molar heat capacities, $C_{p,m}/R$, at constant pressure plotted against temperature T for $WSi_{2.06}$, up to $T = 2200\,K$: (a) Callanan *et al.* [2]; (b) Mezaki *et al.* [4]; (c) Bondarenko *et al.* [5].

arises from the vibration of the atoms in the crystal lattice and produces a dependency on T^3, T^5, T^7... and at very low temperatures, the $C_{p,m} = C_v$. From

$$C_v = \gamma T + aT^3 + bT^5 + \ldots \text{ and} \tag{1}$$

$$C_v/T = \gamma + aT^2 + bT^4 + \ldots, \tag{2}$$

the electronic component is determined from a plot of $C_{p.m}/T$ against T^2 as $T \rightarrow 0$ or the more sensitive $(C_{p,m}-\gamma \cdot T)/T^3$ against T^2. The intercept of the $C_{p.m}/T$ or $(C_{p,m}-\gamma \cdot T)/T^3$ plot is the γ, the electronic component of the heat capacity. Shown in Figs 13, 14 and 15 are the plots for the materials W $Si_{2.06}$, Mo $Si_{2.067}$, and W Te_2, respectively. The values of the γ in Table 1 were obtained by multiplying the values at the intercepts in Figs 13, 14 and 15 by the gas constant R. The value of γ obtained by Lasjaunais *et al.* [20] based on heat pulse measurements from $0.2 \leq (T/K) \leq 7$ for Mo Si_2 is also shown in Table 1.

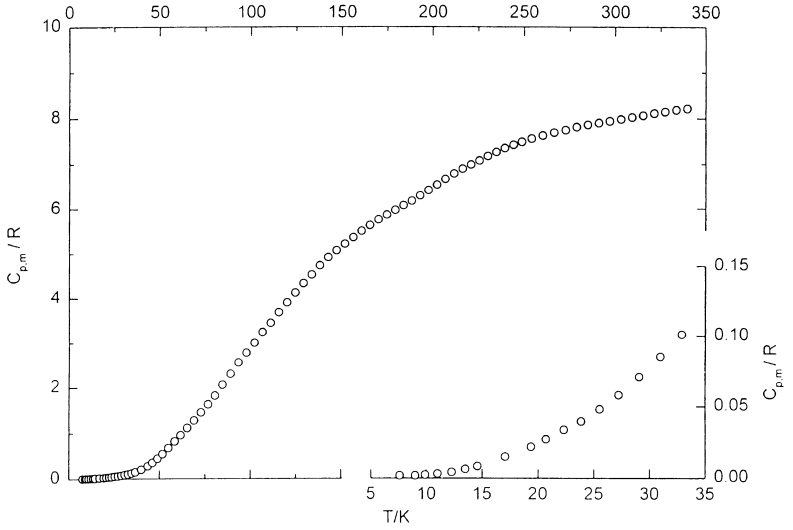

Fig. 7 Experimental molar heat capacities, $C_{p,m}/R$, at constant pressure plotted against temperature T for $MoSi_{2.067}$. The region below $T = 35\,K$ is enlarged in the lower right-hand corner.

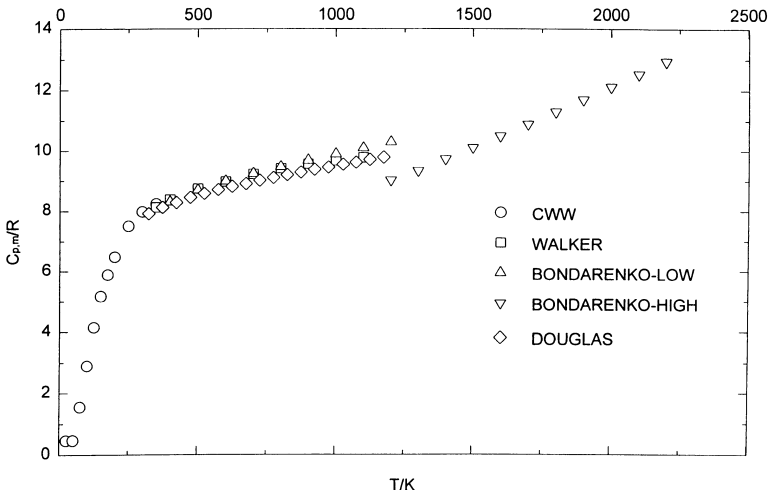

Fig. 8 Experimental molar heat capacities at constant pressure, $C_{p,m}/R$, of molybdenum disilicide to $T = 2200$ K. ◇, Douglas & Logan [9]; □, Walker *et al.* [10]; △, Bondarenko *et al.* [11]; ▽, Bondarenko *et al.* [5]; ○, Callanan *et al.* [6].

CONCLUDING COMMENTS

Tungsten disilicide, WSi_2, has no structural phase transition over the temperature region $0 \leq (T/\mathrm{K}) \leq 1200$ and its tetragonal D^{17}_{4h} space group remains unchanged over this interval. The material remains stable up to $T = 2400$ K, melts around $T = 2437$ K, and proves to be an excellent engineering material. In the same family of transition metal silicides, molybdenum disilicide $MoSi_2$ exhibits similar behaviour in its thermodynamic properties and crystal structure. It also retains its D^{17}_{4h} space group over the range $0 \leq (T/\mathrm{K}) \leq 2200$ and proves to be an excellent engineering material stable to $T = 2200$ K. However, our knowledge of the thermodynamic properties of other members of this family are sparse.

Tungsten ditelluride has no structural phase transition between $0 \leq (T/\mathrm{K}) \leq 326$ and its orthorhombic D^{16}_{2h} space group remains over this temperature range. The heat capacity anomaly is believed due to

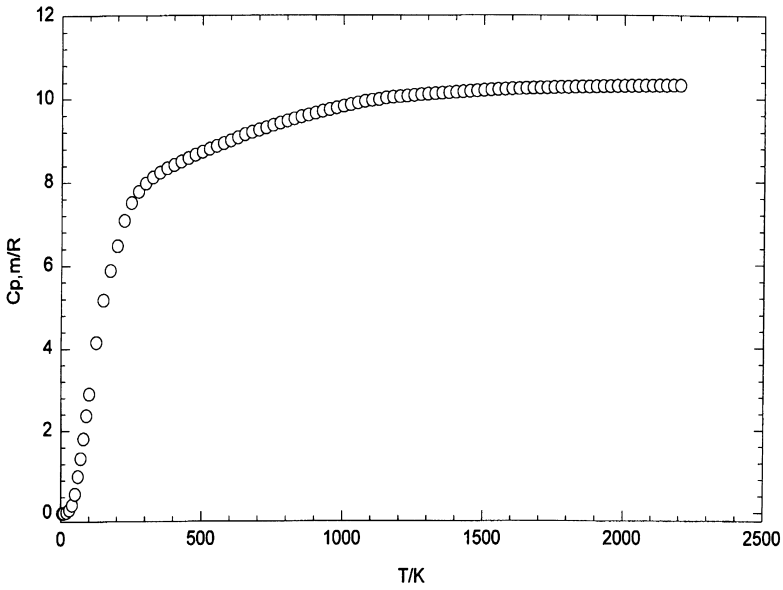

Fig. 9 Estimated molar heat capacities, $C_{p,m}/R$, at constant pressure plotted against temperature to $T = 2200$ K for $MoSi_{2.067}$.

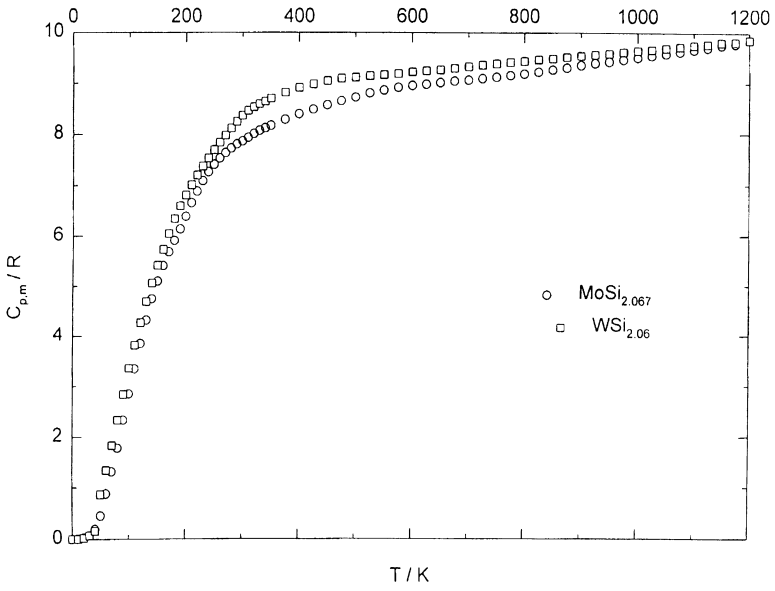

Fig. 10 Comparison of molar heat capacities at constant pressure, $C_{p,m}/R$, plotted against temperature from $T \rightarrow 0$ to $T = 1200\,K$ for: □, $MoSi_{2.067 \pm 0.002}$, and ○, $Wsi_{2.06}$.

anisotropy, possible in the electrical conductivity. Unfortunately thermodynamic properties are unknown at $T \geq 326\,K$ for tungsten ditelluride and other members of this family of layered transition metal chalcogenides. The absence of thermodynamic information handicaps our efforts to assess their full usefulness as engineering materials especially at elevated temperatures.

This IUPAC sponsored 15th International Conference on Chemical Thermodynamics, ICCT-98, is the last to occur in this millennium, and given the rapidly evolving field of materials, it is important to consider the question where is the field of the field of thermodynamics headed and where should it be headed.

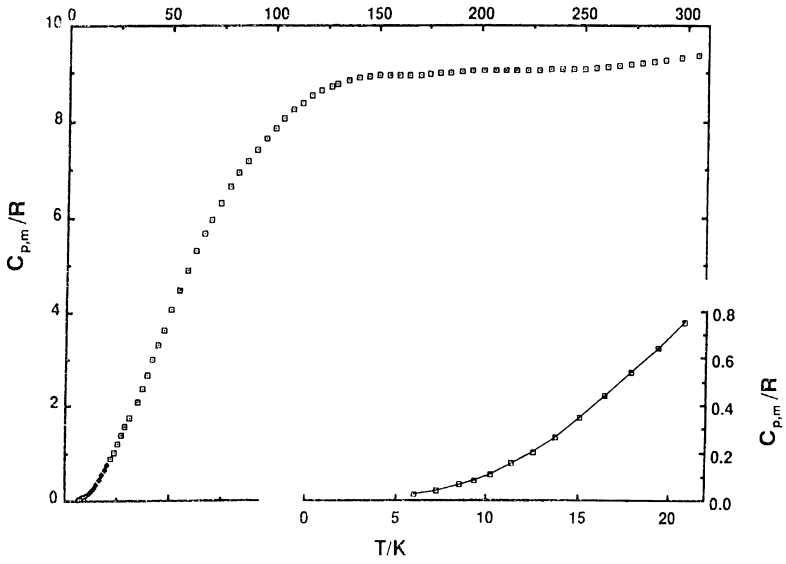

Fig. 11 Experimental molar heat capacities, $C_{p,m}/R$, at constant pressure plotted against temperature T for WTe_2, The region below $T = 23\,K$ is enlarged in the lower right-hand corner.

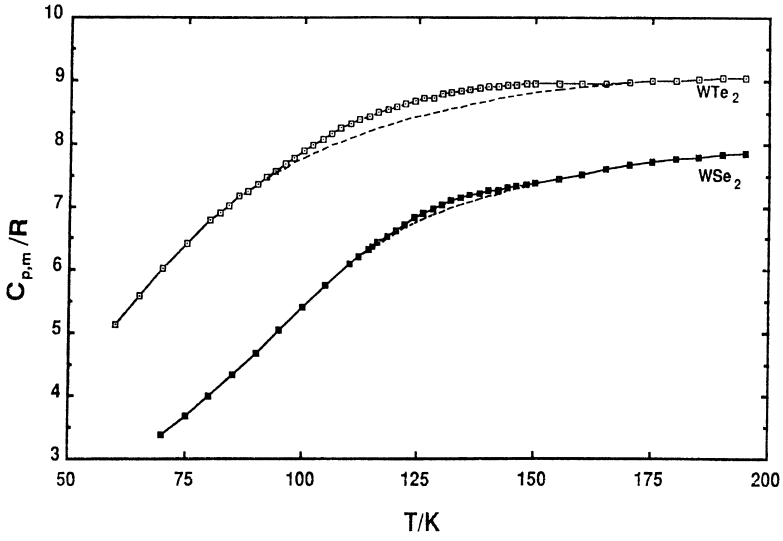

Fig. 12 Comparison of the experimental heat capacities, $C_{p,m}/R$, at constant pressure plotted against temperature T for tungsten disilicide and tungsten diselenide. The points are experimental values and the dashed line represents the lattice heat capacity.

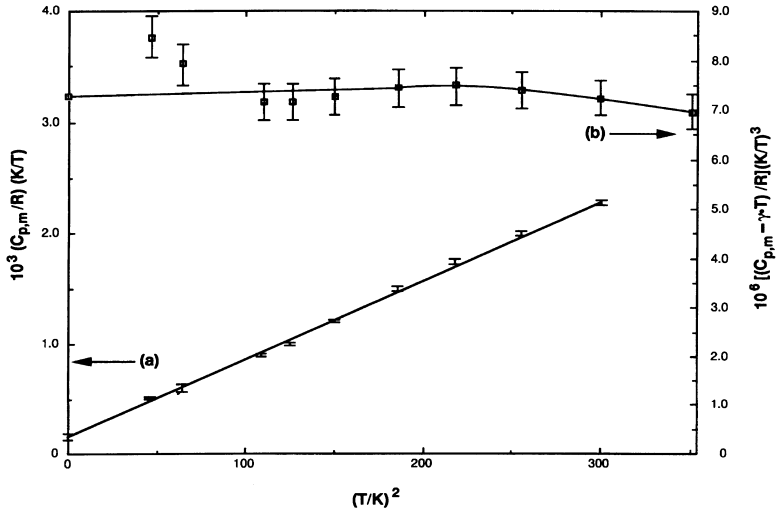

Fig. 13 Plots of (a) $C_{p,m}/(RT)$ and (b) $(C_{p,m} - \gamma T)/(RT^3)$ against T^2 for $WSi_{2.06}$, The vertical error bars correspond to: (a) $0.05(C_{p,m}/R)(K/T)$ and (b) $0.10\{(C_{p,m} - VT)/R\}(K/T)$.

Table 1 Comparison of γ values (γ, $mJ/K^2/mol$)

Cu	0.744
Al	1.21
W	1.36
Mo	2.11
$MoSi_{2.067}$	0.54
$MoSi_2$	0.57 [10]
WC	0.79
$Wsi_{2.06}$	1.33
WTe_2	5.99

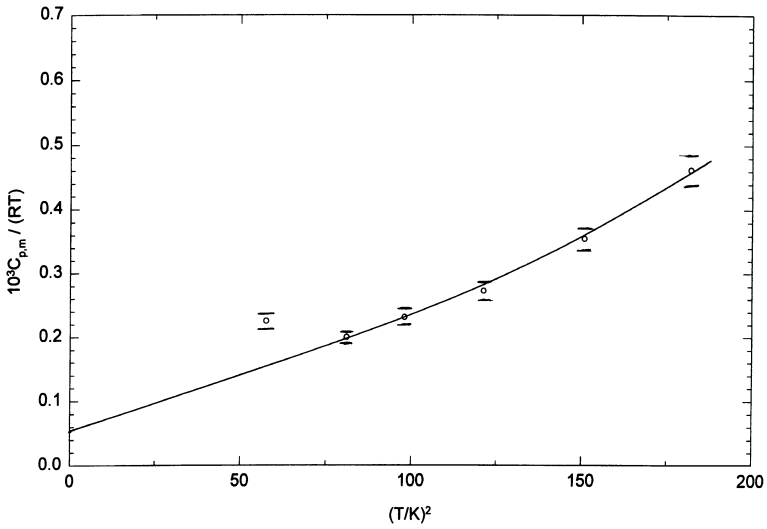

Fig. 14 Plot of $C_{p,m}/(RT)$ against T^2 for for $MoSi_{2.067}$. Error bars correspond to $0.10(C_{p,m}/R)(10^3 \cdot K/T)$.

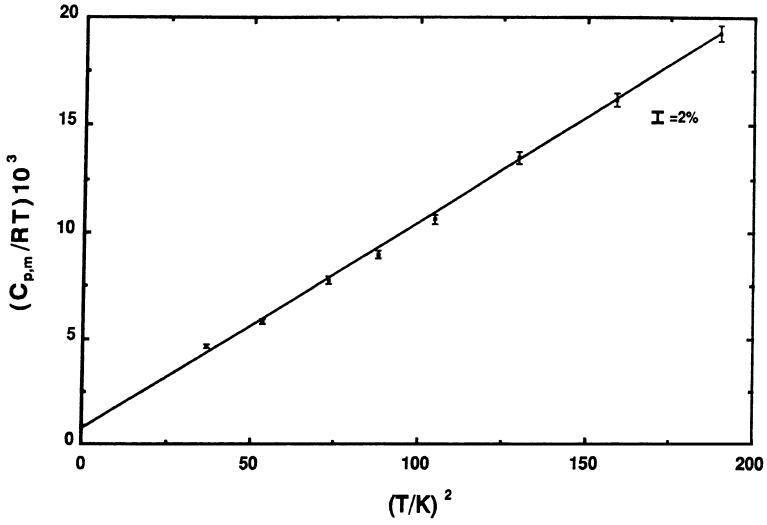

Fig. 15 Plot of $C_{p,m}/(RT)$ against T^2 for WTe_2. Error bars correspond to $0.02(C_{p,m}/R)(10^3 \cdot K/T)$.

REFERENCES

1 T. B. Massalski, L. H. Bennett, J. L. Murray, H. Baker. *Binary Alloy Phase Diagrams*, pp. 1588, 1632, 2063, 2118. ASM International, Materials Park, OH (1986).

2 J. E. Callanan, R. D. Weir, E. F. Westrum Jr. *J. Chem. Thermodyn.* **25**, 1391–1401 (1993), and references therein.

3 J. E. Callanan, R. D. Weir, E. F. Westrum Jr. *J. Chem. Thermodyn.* **28**, 1233–1245 (1996).

4 R. Mezaki, E. W. Tilleux, T. F. Jambois, J. L. Margrave. In *Advances in Thermophysical Properties at Extreme Temperatures and Pressures* (S. Gratch, ed.), pp. 138–144. ASME, New York (1965).

5 V. P. Bondarenko, E. N. Fomichev, A. A. Kalashnik. *Heat Transfer—Soviet Res.* **5**, 76–78 (1973).

6 J. E. Callanan, G. A. Hope, R. D. Weir, E. F. Westrum Jr. *J. Chem. Thermodyn.* **24**, 627–638 (1992), and references therein.

7 (a) P. A. G. O'Hare. *J. Chem. Thermodyn.* **19**, 675–701 (1987); (b) P. A. G. O'Hare, G. A. Hope. *J. Chem. Thermodyn.* **24**, 639–647 (1992).

8 O. Thomas, J. P. Senateur, R. Madar, O. Laborde, E. Rosencher. *Solid State Commun.* **55**, 629–632 (1985).

9 T. B. Douglas, W. M. Logan. *J. Res. Natl. Bur. Stand (US)* **53**, 91–93 (1954).

10 B. E. Walker, J. A. Grand, R. R. Miller. *J. Phys Chem.* **60**, 231–233 (1956).

11 V. P. Bondarenko, P. N. B'yugov, V. I. Zmii, A. S. Kuyazhev. *Teplofiz. Vys. Temp.* **10**, 1013–1017 (1972).

12 A. S. Bolgar, Zh. A. Trofima, A. A. Yanaki. *Poroshk. Metall.* **5**, 53–56 (1990).

13 R. D. Weir, L. A. K. Staveley. *J. Chem. Phys.* **73**, 1386–1392 (1980).

14 R. J. C. Brown, J. E. Callanan, R. D. Weir, E. F. Westrum Jr. *J. Chem. Thermodyn.* **18**, 787–792 (1986).

15 R. J. C. Brown, J. E. Callanan, R. D. Weir, E. F. Westrum Jr. *J. Chem. Phys.* **85**, 5963–5970 (1986).

16 R. J. C. Brown, J. E. Callanan, T. E. Haslett, R. D. Weir, E. F. Westrum Jr. *J. Chem. Thermodyn.* **19**, 711–716 (1987).

17 R. J. C. Brown, J. E. Callanan, T. E. Haslett, R. D. Weir, E. F. Westrum Jr. *J. Chem. Thermodyn.* **19**, 1111–1116 (1987).

18 R. J. C. Brown, J. E. Callanan, R. D. Weir, E. F. Westrum Jr. *J. Chem. Thermodyn.* **19**, 1173–1182 (1987).

19 R. J. C. Brown, R. D. Weir, E. F. Westrum Jr. *J. Chem. Phys.* **91**, 399–407 (1989).

20 J. C. Lasjaunais, M. Saint-Paul, O. Laborde, O. Thomas, J. P. Senateur, R. Madar. *Phys. Rev. B.* **37**, 364–366 (1988).

21 T. Letcher. *Thermodynamics in the 21st Century*. Blackwell, Oxford. (1999).